25th ABCM International Congress of Mechanical Engineering
October 20-25, 2019, Uberlândia, MG, Brazil

COB–2019-0178
COMPARISON OF FRF BASED DAMAGE INDEXES FOR CRACKED BEAMS

Tomé Seichi da Nóbrega Guenka
Marcela Rodrigues Machado
Campus Universitário Darcy Ribeiro, Departamento de Engenharia Mecânica / FT – UnB, asa norte - Brasília / DF
tomeseichi@gmail.com
marcelam@unb.br

Leila Khalij
LMN/INSA de ROUEN Normandie, 76000 Rouen, France
leila.khalij@insa-rouen.fr

Abstract. *This article presents an evaluation of FRF based damage indexes associated with the spectral element method (SEM). Eight indexes were used: FRAC (Frequency Domain Assurance Criterion), FAAC (Frequency Amplitude Assurance Criterion), GSC (Global Shape Criterion), GAC (Global Amplitude Criterion), Monnier's and Banerjee's Damage Index (DI), Average Integration GSC/GAC (AIGSC, AIGAC). These were applied to relate the frequency response functions of variably damaged and undamaged beams. The results were then compared to determine the best-suited indexes for damage detection and size evaluation.*

Keywords: *Damage Index, Frequency Response Function, Spectral Element Method, Structural Health Monitoring.*

1. INTRODUCTION

The structures developed by the aerospace, mechanical and civil industries may be subject to aggressive environments and conditions, such as corrosion, high pressure and temperature, rough weather/natural disasters and overload. Frequently, such environments and conditions provoke structural deterioration that will eventually lead critical systems to failure. Many methods were developed to analyze damage occurs due to degradation of the structure, while other approaches focus on damage detection and structural monitoring. Damage may induce a change of the local and global properties of a structure. These changes are included in the dynamic response signal obtained from the structure and, under control, they may be associated with damage parameters. Many damage detection techniques were developed in the last decades; some can be grouped based on modal data; electromechanical impedance; static parameter; acoustic emission; and wave-based approaches (Su and Ye, 2009).

Methods based on modal or vibrational data (frequency response functions, modal shape and modal damping) are built from the fact that the presence of structural damage reduces structural stiffness, dislocates natural frequencies and alters the modes of vibration and the frequency response functions. These alterations happen as modal parameters are functions of the physical properties of the structure (mass, damping and stiffness). Thus, changes in such physical properties will cause a detectable change in the modal properties (Doebling et al.., 1998). Damage evaluation based on these changes can be challenging, mainly when applied to complex structures. For that reason, methods for the examination of the changes in the structural vibration characteristics were developed. Modifications of the modal properties are used as damage indicators. Advantages and uses of this method are its simplicity and low cost and effectiveness for the detection of significant damage in large structures or rotary machines. The inconveniences are the lack of sensibility to small damage or its propagation, the need for many measurement points, and the method is hypersensitive to the boundary and environment changes.

To classify damage, it is necessary to observe the effects of damage in a structure. Damage may be classified as linear or non-linear (Doebling et al., 1998). Linear structural damage is observed when the initially linear-elastic structure remains linear-elastic after damage, and the structural response can still be modelled using linear equations. Non-linear damage is observed when an initially linear-elastic structure behaves in a non-linear manner after the introduction of damage (e.g. fatigue cracks). Identification methods can also be classified according to four levels of damage identification: 1) detection of damage present in the structure; 2) determination of the geometrical damage location; 3) quantification of the severity of the damage, and 4) prediction of the remaining structure lifespan. Another classification category for damage identification makes a distinction between methods for the detection of damage caused by extreme events and techniques used for continuous structural performance monitoring (Morassi and Vestroni, 2008).

The alterations caused to the structural dynamic response are often used as damage indicators when compared to the original response. This study compares frequency response function based damage indicators (DI), nine in total: Frequency Response Assurance Criterion (FRAC), Frequency Amplitude Assurance Criterion (FAAC), Global Shape Criterion (GSC), Global Amplitude Criterion (GAC), Monnier's Damage Index (DI) (Monnier, 2006) and Average Integration GSC/GAC (AIGSC, AIGAC). The damaged structure (Krawczuk, 2002) and undamaged structure are modelled using the Spectral Element Method (SEM) for a beam. FRF's were obtained for the damaged and undamaged beam. Damage evaluation is given by DI's (Sinou, 2009; Zang, 2001; Monnier, 2006), and this study's objective is to find a better suited DI for future applications associated with SEM. The damage indicators are applied and compared according to each DI efficiency in detecting damage and estimating its size.

2. SPECTRAL ELEMENT METHOD

The Spectral Element Method is similar to the Finite Element Method, though with two essential differences: the SEM formulation is written in the frequency domain, and the element interpolation function is the analytical solution of the wave equation. Based on the later characteristic/difference, the number of elements required for a spectral model will be the same as the number of discontinuities in the structure.

2.1 Beam Espectral Element

For the wave propagation analysis in a beam, consider a slender beam under the Euler Bernoulli theory, with an applied transverse load. Assuming small transverse and rotational displacements and disregarding the deformation caused by shearing, the movement differential equation written in the frequency domain (Doyle, 1997) is given by:

$$\frac{d^4v}{dx^4} - k^4 v = F \tag{1}$$

Whose homogenous equation solution is given by:

$$\hat{v}(x,t) = Ae^{-ik_1 x} + Be^{-ik_2 x} + Ce^{ik_1(L-x)} + De^{k_2(L-x)} \tag{2}$$

where $\hat{v}$ is the transverse displacement in the frequency domain, F is the external force e L is the beam's length. The wave numbers are given by:

$$k \equiv \sqrt{\frac{\omega^2 \rho S}{EI}};\ k_1 = \pm k;\ k_2 = \pm ik \tag{3}$$

where ω is the circular frequency, E is the beam's Young Modulus, S is the cross-sectional area, ρ is the material's density, I is the moment of inertia and $i = \sqrt{-1}$. Using the complex Young modulus, $E_c = E(1 + i\eta)$, an internal structural damping is introduced. Then, η is the hysteretic damping loss factor.

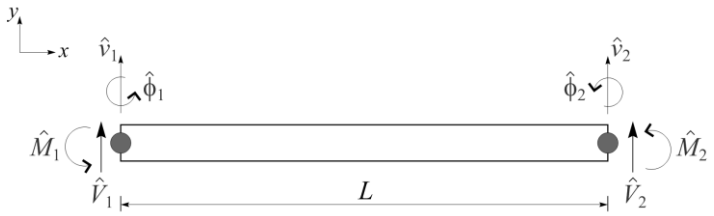

Figure 1. Beam Spectral Element with two knots.

Figure 1 illustrates a healthy beam element with two knots, two degrees of freedom per knot ($\hat{v}$ e $\hat{\phi}$) and two nodal loads ($\hat{V}$ e $\hat{M}$). Applying the displacements and nodal rotations from the Fig. 1 Element to Eq. (2), the coefficients A, B, C and D can be obtained. Replacing these coefficients again on Eq. (2), the equation for the calculation of the displacements and rotations in any arbitrary point of the beam may be written as:

$$\hat{v}(x) = \hat{g}_1(x)\hat{v}_1 + \hat{g}_2(x)\hat{\phi}_1 + \hat{g}_3(x)\hat{v}_2 + \hat{g}_4(x)\hat{\phi}_2 \tag{4}$$

where $\hat{g}_i(x)$ are wave shape functions defined by Doyle (1997):

$$\hat{g}_1(x) = \left[r_1\hat{h}_1(x) + r_2\hat{h}_2(x)\right]/\Delta$$

$$\hat{g}_2(x) = \left[r_1\hat{h}_3(x) + r_2\hat{h}_4(x)\right]/\Delta$$
$$\hat{g}_3(x) = \left[r_1\hat{h}_2(x) + r_2\hat{h}_1(x)\right]/\Delta$$
$$\hat{g}_4(x) = \left[r_1\hat{h}_4(x) + r_2\hat{h}_3(x)\right]/\Delta \quad (5)$$

where:

$$\Delta = -r_1^2 + r_2^2$$

$$r_1 = i(k_1 - k_2)(1 - e^{-ik_1L}e^{-ik_2L})$$
$$r_2 = i(k_1 + k_2)(1 - e^{-ik_1L}e^{-ik_2L})$$

$$\hat{h}_1(x) = ik_2\left(e^{-ik_1x} - e^{-ik_2L}e^{-ik_1(L-x)}\right) - ik_1(e^{-ik_2x} - e^{-ik_1L}e^{-ik_2(L-x)})$$
$$\hat{h}_2(x) = ik_2\left(e^{-ik_2L}e^{-ik_1x} - e^{-ik_1(L-x)}\right) + ik_1(e^{-ik_1L}e^{-ik_2x} - e^{-ik_2(L-x)})$$
$$\hat{h}_3(x) = \left(e^{-ik_1x} + e^{-ik_2L}e^{-ik_1(L-x)}\right) - (e^{-ik_2x} - e^{-ik_1L}e^{-ik_2(L-x)})$$
$$\hat{h}_4(x) = \left(e^{-ik_2x}e^{-ik_1L} + e^{-ik_1(L-x)}\right) - (e^{-ik_1x}e^{-ik_2L} + e^{-ik_1(L-x)})$$

Using the relation between the knots nodal loads and degrees of freedom, and applying the SEM boundary conditions, we obtain:

$$\begin{pmatrix} \hat{V}_1 \\ \hat{M}_1 \\ \hat{V}_2 \\ \hat{M}_2 \end{pmatrix} = \hat{K} \begin{pmatrix} \hat{v}_1 \\ \hat{\phi}_1 \\ \hat{v}_2 \\ \hat{\phi}_1 \end{pmatrix} \quad (6)$$

where $\hat{K}$ is the dynamic stiffness matrix of the healthy beam spectral element. The matrix is symmetric and complex, and can be expressed as:

$$\hat{K} = \frac{EI}{L^3}\begin{bmatrix} 1 & 1 & e^{-ikL} & e^{-kL} \\ -ik & -k & ike^{-ikL} & ke^{-kL} \\ e^{-ikL} & e^{-kL} & 1 & 1 \\ -ike^{-ikL} & -ke^{-kL} & ik & k \end{bmatrix} \quad (7)$$

2.2 Cracked Beam Spectral Element

The spectral element of a beam with a transversal non-propagating crack (Krawczuk, 2002) is illustrated in Fig. 2. The element contains twos nodes with two degrees of freedom (dof) each, where "L" is the length, "L_1" is the crack position relative to node 1 and "a" is the length (depth) of the crack. The crack is modeled by a local dimensionless flexibility represented by "θ" which is calculated by the Castigliano theorem and fracture mechanics law (Tada et al., 1973).

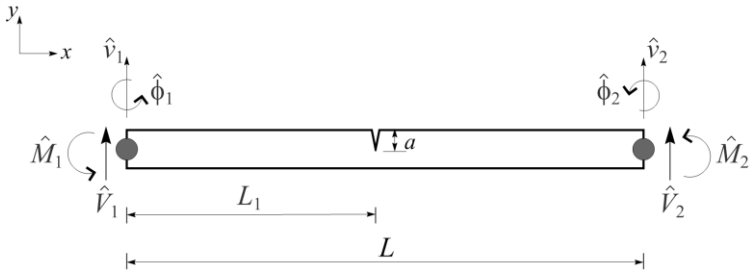

Figure 2: Cracked Beam Spectral Element with two nodes.

For the cracked beam, the solution of Eq. (2) is given by two equations, presented in Eq. (8):

$$\hat{v}^l(x) = A_1e^{-i(k_1x)} + B_1e^{-(k_2x)} + C_1e^{-ik_1(L_1-x)} + D_1e^{-k_2(L_1-x)}$$
$$\hat{v}^r(x) = A_2e^{-ik_1(L_1+x)} + B_2e^{-k_2(L_1+x)} + C_2e^{-ik_1(L-(L_1+x))} + D_2e^{-k_2(L-(L_1+x))} \quad (8)$$

where $\hat{v}^l$ and $\hat{v}^r$ are the vertical displacements to the left and to the right of the crack, respectively. The $A_1; B_1; C_1; D_1; A_2; B_2; C_2$ and D_2 coefficients are determined by boundary conditions. From the displacement and nodal

loads, the stiffness matrix is obtained in a similar fashion to the healthy beam spectral element. However, the dynamic stiffness matrix of the cracked beam spectral element is written as:

$$\widehat{K}_c = \frac{EI}{L^3}\begin{bmatrix} 1 & 1 & a & b & 0 & 0 & 0 & 0 \\ -ik & -k & ika & kb & 0 & 0 & 0 & 0 \\ -a & -b & -1 & -1 & a & b & c & d \\ iak - a\theta k^2 & bk + b\theta k^2 & -ik - \theta k^2 & -k + \theta k^2 & ika & -kb & ikc & kd \\ -k^2 a & k^2 b & -k^2 & k^2 & k^2 a & -k^2 b & k^2 c & -k^2 d \\ ik^3 a & -k^3 b & -ik^3 & k^3 & -k^3 a & k^3 b & ik^3 c & -k^3 d \\ 0 & 0 & 0 & 0 & f & g & 1 & 1 \\ 0 & 0 & 0 & 0 & -ikf & -kg & ik & k \end{bmatrix} \tag{9}$$

where: $\mathrm{a} = \mathrm{e}^{\mathrm{ikL_1}}, \mathrm{b} = \mathrm{e}^{-\mathrm{kL_1}}, \mathrm{c} = \mathrm{e}^{-\mathrm{ik(L-L_1)}}, \mathrm{d} = \mathrm{e}^{\mathrm{k(L-L_1)}}, \mathrm{f} = \mathrm{e}^{-\mathrm{ikL}}, \mathrm{g} = \mathrm{e}^{-\mathrm{kL}}$.

2.3 Local beam flexibility at the crack position

The flexibility coefficient of crack "θ" is obtained using Castigliano's method, where flexibility at the crack position for a spectral element of single dimension beam may be obtained by:

$$\mathrm{c} = \frac{\partial^2 U}{\partial \mathrm{P}^2} \tag{10}$$

where "U" denotes the elastic deformation energy due to the crack and P is nodal load on the element. Considering that only the first crack mode is present in the beam element, the elastic deformation energy may be expressed as:

$$\mathrm{U} = \frac{1 - \nu\hat{}2}{E} \int_{\mathrm{Sc}} \mathrm{K}_I^2 \, \mathrm{dS}_c \tag{11}$$

where "ν" is Poisson's ratio, "S_c" is the cracked area and "K_I" is a stress intensity factor correspondent to the crack mode I that may be represented by:

$$\mathrm{K_I} = \mathrm{c}\,\frac{6\mathrm{M}}{\mathrm{bh}^2}\sqrt{\pi\alpha}\,\mathrm{f}\frac{\alpha}{\mathrm{h}} \tag{12}$$

where "b" is the base and "h" is the height of the cross section of the beam; "α" is the variation of crack depth; "M" is the bending moment at the crack position and "f" is a correction function of the stress intensification factor of the mode I that is written as:

$$f\left(\frac{\alpha}{h}\right) = \sqrt{\left\{\frac{2\mathrm{h}}{\pi\alpha}\tan\left(\frac{\pi\alpha}{2\mathrm{h}}\right)\right\}\frac{0.923 + 0.199\left(1 - \sin(\pi\alpha\backslash 2\mathrm{h})\right)^4}{\cos(\pi\alpha\backslash 2\mathrm{h})}} \tag{13}$$

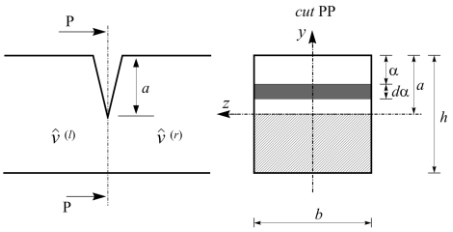

Figure 3: Cross-section of a cracked beam at the crack position.

The "*c"* coefficient used to obtain the crack flexibility may be written in the following way:

$$c = \frac{72\pi}{bh^2}\int_0^{\bar{a}} \bar{\alpha}\, f^2(\bar{\alpha}) d\bar{\alpha} \tag{14}$$

where $\bar{a} = a/h$ and $\bar{\alpha} = \alpha/h$. Local dimesionless flexibility is given by:

$$\theta = \frac{EI\ c}{L} \tag{15}$$

3. DAMAGE INDEX METHOD

The evaluated damage detection methods were all damage indexes based on the Frequency Response Function (FRF) of the beams (damaged and undamaged). The FRF may be defined as:

$$H_{ij}(\omega) = \frac{X_i}{F_j} \tag{16}$$

where X_i is the response on the "i" coordinate and F_j is the excitation on the "j" coordinate for different "ω" frequencies. The stiffness and the damping of a structure are influenced by the presence of damage (crack), thus modifying the responses of the structure. The indexes compare the FRF's of the cracked and healthy beams and should indicate the size of the crack, since the size of the crack directly influences the changes in the FRF of a structure. Of the nine indexes evaluated in this study, two are extensions of the Modal Assurance Criterion (MAC) in the frequency domain (Sinou, 2009): the Frequency Response Assurance Criterion (FRAC), Eq. (17) and the Frequency Amplitude Assurance Criterion (FAAC), Eq. (18).

$$FRAC_{ij}(\omega) = \frac{\left|H_{ij}^{damaged}(\omega)(H_{ij}^{undamaged}(\omega))^*\right|^2}{H_{ij}^{undamaged}(\omega)(H_{ij}^{undamaged}(\omega))^* H_{ij}^{damaged}(\omega)(H_{ij}^{damaged}(\omega))^*} \tag{17}$$

$$FAAC_{ij} = \frac{2\left|H_{ij}^{damaged}(\omega)(H_{ij}^{undamaged}(\omega))^*\right|}{\{(H_{ij}^{damaged}(\omega))(H_{ij}^{damaged}(\omega))^*\}+\{(H_{ij}^{undamaged}(\omega))(H_{ij}^{undamaged}(\omega))^*\}} \tag{18}$$

where "*" represents the Hermitian transpose, "$H_{ij}^{damaged}(\omega)$" is the FRF vector on "j" for the damaged beam excited on "i" and "$H_{ij}^{undamaged}(\omega)$" is the FRF vector for the healthy beam, on the same aforementioned coordinates. Both DI's return a value between zero and one: the closest it is to one, the smaller is the damage, and a value equal to one represents a completely undamaged beam. Both FRAC and FAAC give information on the beam health in a determined position based on amplitude.

Two other functions were utilized as damage indexes: The Global Shape Criterion (GSC) and the Global Amplitude Criterion (GAC) (Zang, 2001), presented in Eq. (19) and Eq. (20).

$$\mathrm{GSC}(\omega) = \frac{\left|H_{undamaged}^*(\omega)H_{damaged}(\omega)\right|^2}{(H_{undamaged}^*(\omega)H_{undamaged}(\omega))(H_{damaged}^*(\omega)H_{damaged}(\omega))} \tag{19}$$

$$\mathrm{GAC}(\omega) = \frac{2\left|H_{undamaged}^*(\omega)H_{damaged}(\omega)\right|}{H_{undamaged}^*(\omega)H_{undamaged}(\omega)+H_{damaged}^*(\omega)H_{damaged}(\omega)} \tag{20}$$

where "$H_{damaged}(\omega)$" and "$H_{undamaged}(\omega)$" are the vectors with the FRF's for each frequency "ω" of the damaged and undamaged beams, respectively. Both GAC and GSC should return values between zero and one for all frequencies. Similarly to the FRAC and FAAC criterions, values closer to zero represent less correlation between the FRF's of damaged and undamaged beams, indicating stifness variation caused by damage. Values closer to unit represent a tighter correlation between responses. Besides GAC and GSC, Zang (2003) defines the Averaged Integration of both GAC and GSC functions, defined in Eq. (21).

$$\begin{aligned} AIGSC &= \frac{1}{N_f}\sum_{i=1}^{N_f} GSC(\omega_i) \\ AIGAC &= \frac{1}{N_f}\sum_{i=1}^{N_f} GAC(\omega_i) \end{aligned} \tag{21}$$

Both AIGSC and AIGAC return a single real value between zero and unity, also representing the correlation between the responses of the damaged and undamaged beams.

The last two damage indexes utilised for comparison were Monnier (2006) Damage Index and Banerjee (2009) Damage Index. Like FRAC and FAAC, both Monnier and Banerjee DI's return a single real value between zero and unity for a given frequency band of interest. Nevertheless, in the case of the DI's, values closer to zero represent smaller damage and values closer to one represent higher damage, that is: zero shows a complete correlation between responses and indicates a healthy or undamaged beam, and one would show no correlation between responses, indicating complete rapture of the beam. Equation (22) shows Monnier's DI (MDI) and Eq. (23) shows Banerjee's DI (BDI).

$$DI = \frac{\sum_{i=1}^{n}\left|H_{ij}^{undamaged}(\omega) - H_{ij}^{damaged}(\omega)\right|}{\sum_{i=1}^{n}\left|H_{ij}^{undamaged}(\omega)\right|} \tag{22}$$

$$DI = \left|1 - \frac{\left|H_{ij}^{damaged}(\omega)\right|^{T} * H_{ij}^{damaged}(\omega)}{\left|H_{ij}^{undamaged}(\omega)\right|^{T} * H_{ij}^{undamaged}(\omega)}\right| \tag{23}$$

where "T" indicates the transpose of the FRF vector. It is necessary to mention that, for this paper, Eq.(23) subtraction operation in the numerator had to be replaced by a sum in order to show values in the expected range.

4. RESULTS AND DISCUSSION

The simulated system is a free-free beam modelled by 2 nodes SEM. The beam is excited with a harmonic force applied on node no. 1, and the response is obtained for both nodes no.1 and no.2. The dimensions and properties set for the beam are $L = 1\,m$, $h = 0{,}02\,m$, $b = 0{,}02\,m$, $E = 80\,GPa$, $\varepsilon = 0{,}01$ and $\rho = 2700\,kg/m^3$. The crack was positioned at $L_1 = 0.5L$. Five beams were simulated, with increasing damage sizes (relative to the cross-section size of the beam).

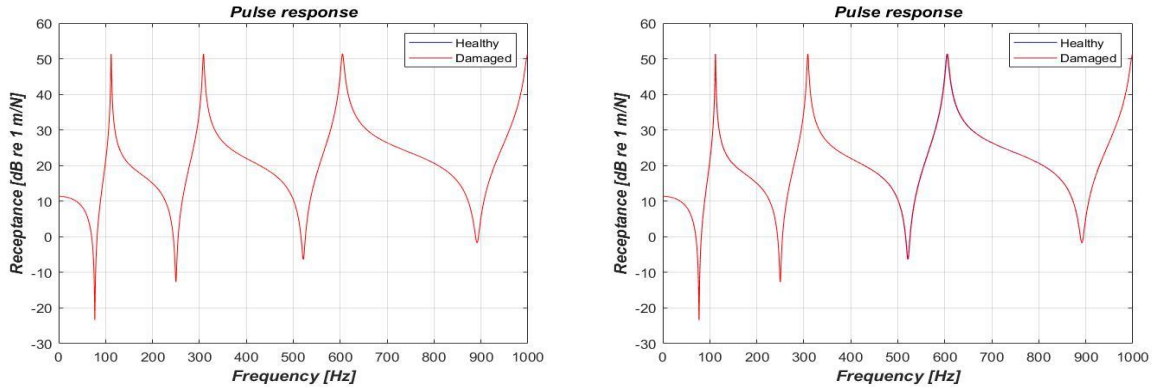

(a)

(b)

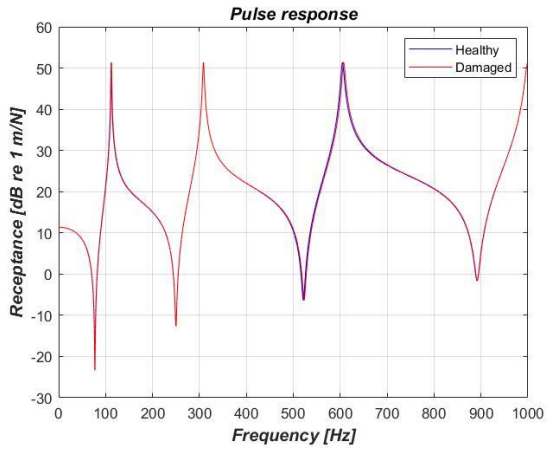

(c)

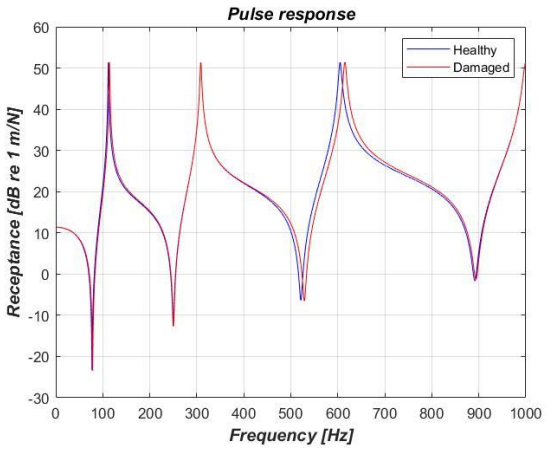

(d)

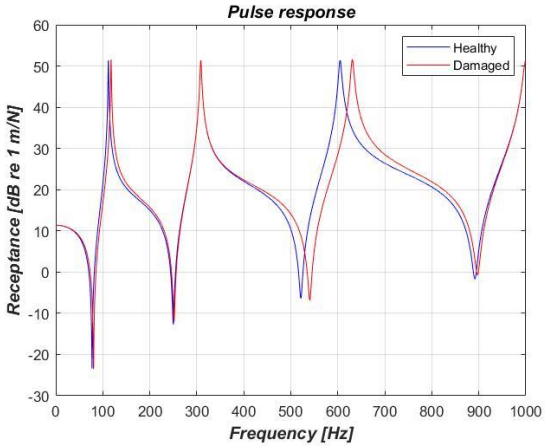

(e)

Figure 4: Comparison of the dynamic responses (FRF) obtained at node no.1 from the healthy beam and cracked beam at different crack levels: a) 1 %; b) 5 %; c)10 %; d) 20 %; e) 30 % relative to the cross-section height.

Figure 4(a-e) shows the FRF's of the cracked and healthy beam obtained at node 1, the same node to be excited. As the severity of the crack grows, the difference between the responses of the undamaged and cracked beam becomes more noticeable. For small damage, between 1~5%, there is little change, mainly on the third mode, and starting from 10 % damage, other modes begin to be affected as well. The comparison of these FRF's allows monitoring the appearance and propagation of a crack. This paper shows the comparison of eight methods to correlate FRF's, which are the GAC, GSC, AIGAC, AIGSC, FRAC, FAAC, Monnier's DI and Banerjee's DI. Through these comparisons, it is possible to obtain damage indicators, enabling a global measure of a structure's integrity.

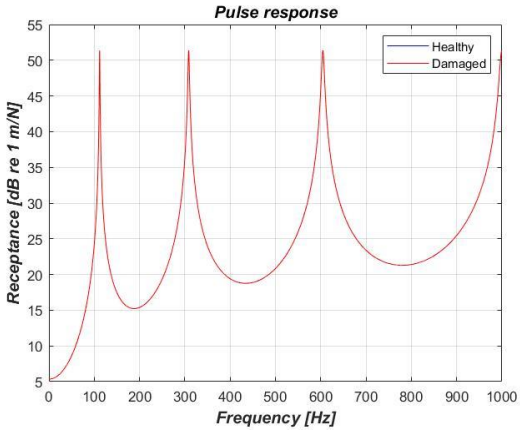

(a)

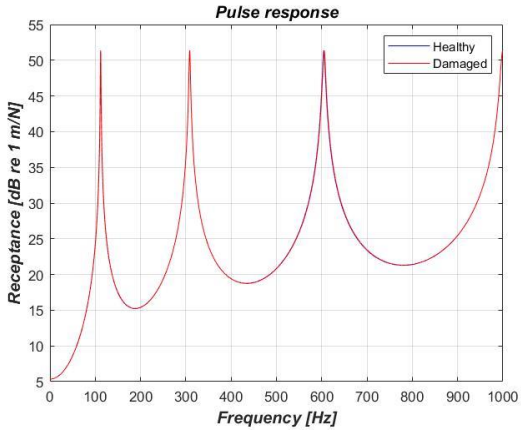

(b)

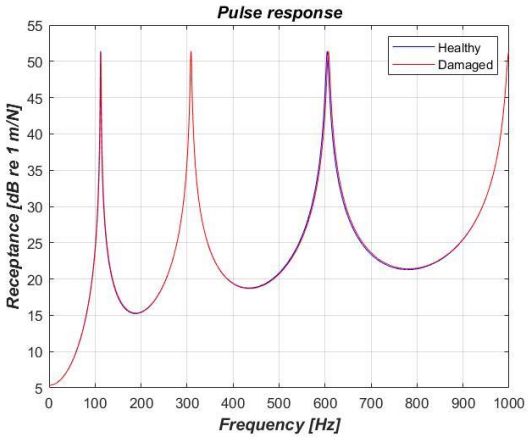

(c)

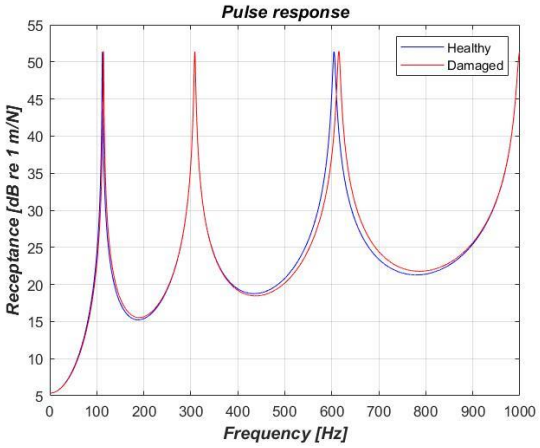

(d)

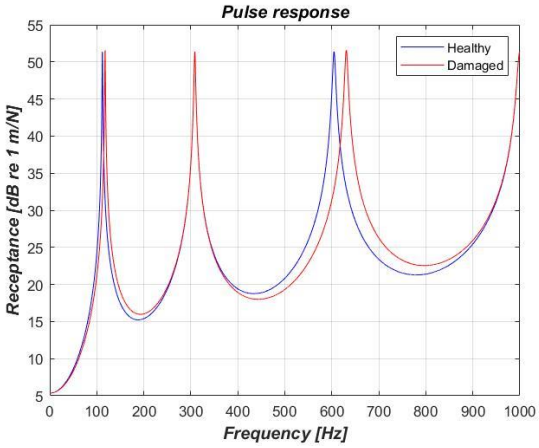

(e)

Figure 5: Comparison of the dynamic responses (FRF) obtained at node no.3 from the healthy beam and cracked beam at different crack levels: a) 1 %; b) 5 %; c)10 %; d) 20 %; e) 30 % relative to the cross-section height.

Figure 5(a-e) shows the FRF's of the cracked and healthy beam obtained at node 2. The responses show similar behaviour to those of node 1, with increasing difference between responses of the undamaged and cracked beams. Figure 6 and Table 1 show the obtained damage indexes were based on the FRF measured on node 1:

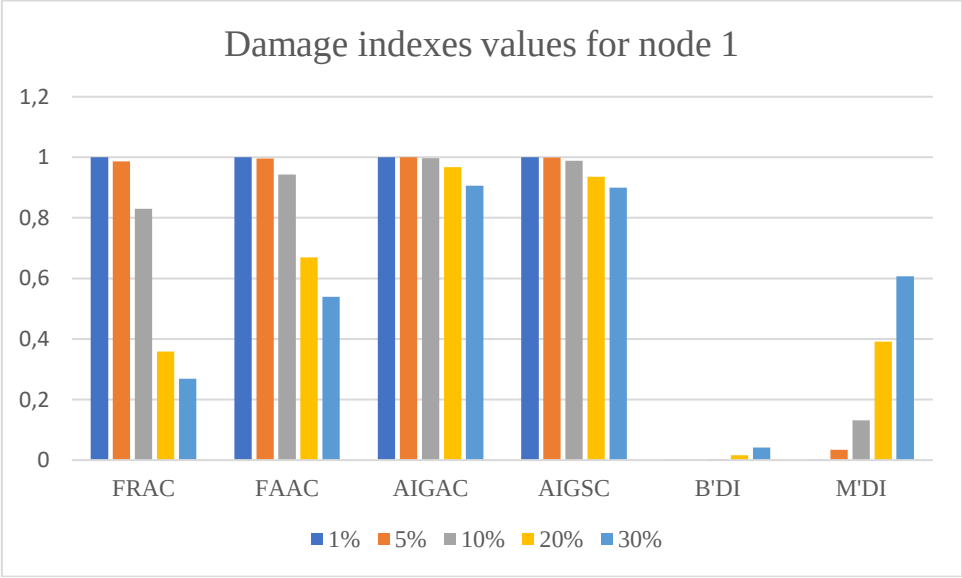

Figure 6: Results of all damage indexes for different damage sizes obtained in node 1.

Table 1: Values of all damage indexes for different damage sizes obtained in node 1.

Damage Size	FRAC	FAAC	AIGAC	AIGSC	B'DI	M'DI
1%	1	1	1	1	3.79E-05	0.0014
5%	0.9866	0.9959	0.9998	0.9992	9.29E-04	0.0344
10%	0.8302	0.9432	0.9969	0.9888	0.0037	0.1313
20%	0.3586	0.6691	0.9677	0.9363	0.0157	0.3914
30%	0.2684	0.5399	0.9063	0.9003	0.0417	0.6067

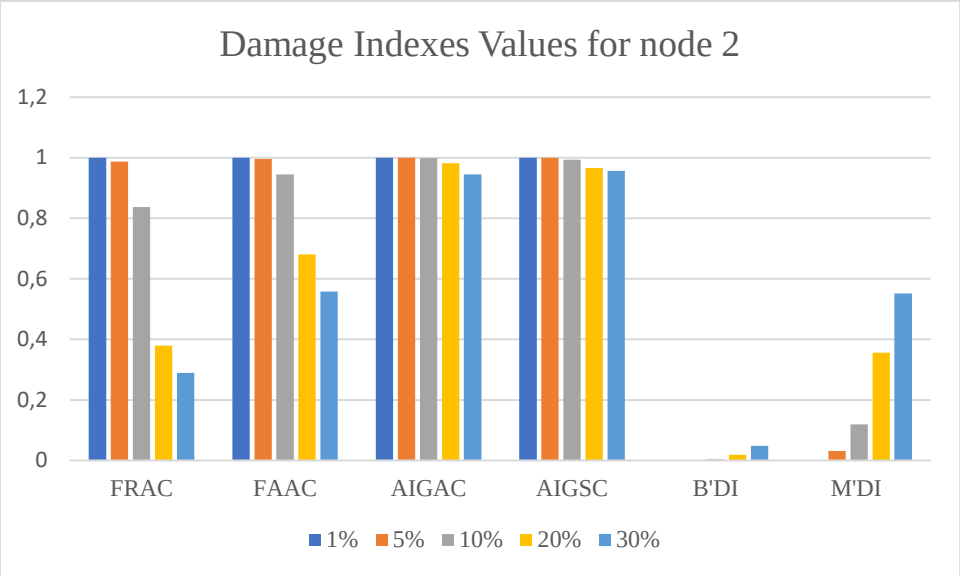

Figure 7: Results of all damage indexes for different damage sizes obtained in node 2.

Table 2: Values of all damage indexes for different damage sizes obtained in node 2.

Damage Size	FRAC	FAAC	AIGAC	AIGSC	B'DI	M'DI
1%	1	1	1	1	4.41E-05	0.0013
5%	0.9872	0.996	0.9999	0.9995	0.0011	0.0313
10%	0.8374	0.9447	0.9982	0.9932	0.0043	0.1193
20%	0.3797	0.6803	0.9813	0.966	0.0183	0.3557
30%	0.2894	0.5582	0.9452	0.9563	0.0483	0.5514

Figures 6,7 and Tables 1,2 show the behaviour of all indexes in both beam nodes. All results obtained correspond to the expected result. It can be seen that the FRAC and FAAC show larger decreases in value as the crack size grows. The indexes AIGAC and AIGSC also show a decrease in value proportional to crack growth, even though more conservative. MDI and BDI have an increment in value as the crack size grow, although MDI values are higher and have a higher increase in value. All methods were efficient in showing the presence of damage, notwithstanding the impossibility of prediction of which modes suffer the most change due to damage, or estimating the damage size or its location.

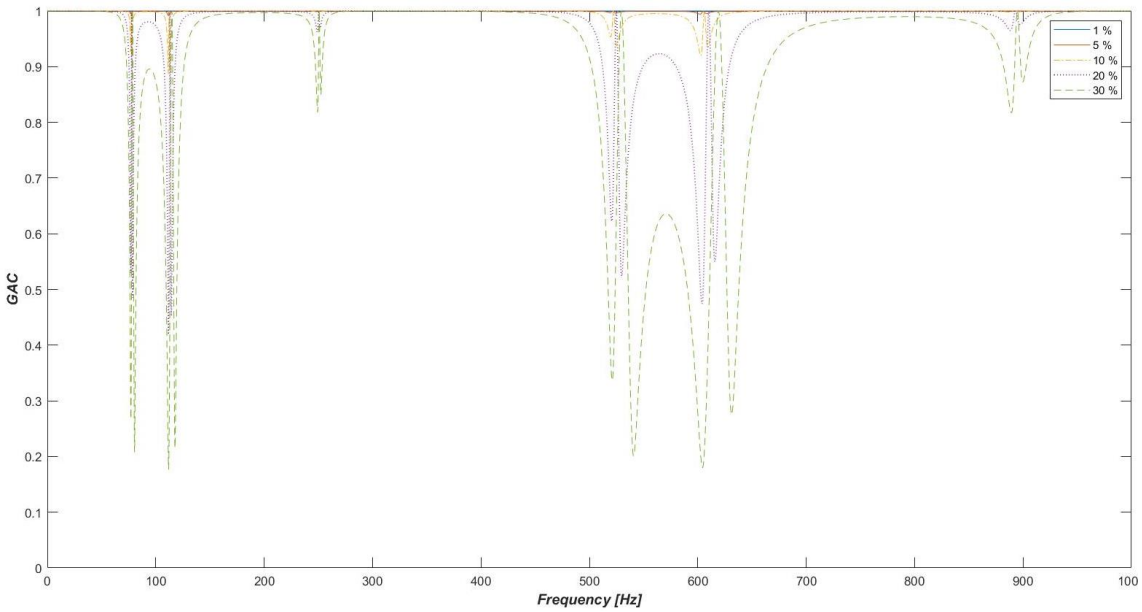

Figure 8: GAC for different crack sizes at node 1.

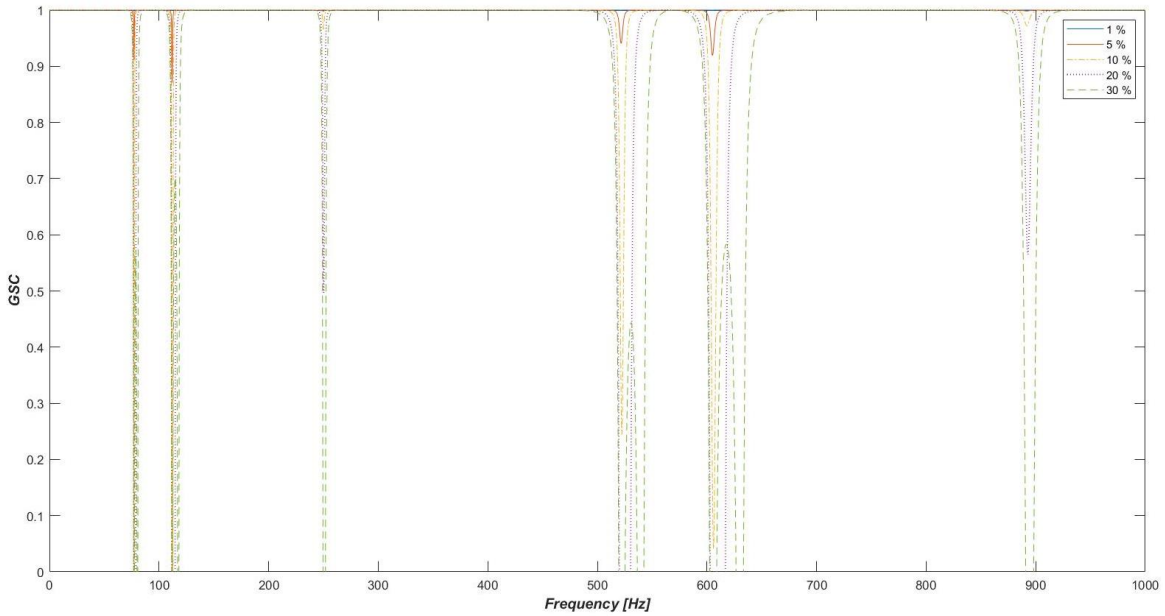

Figure 9: GSC for various crack sizes at node 1.

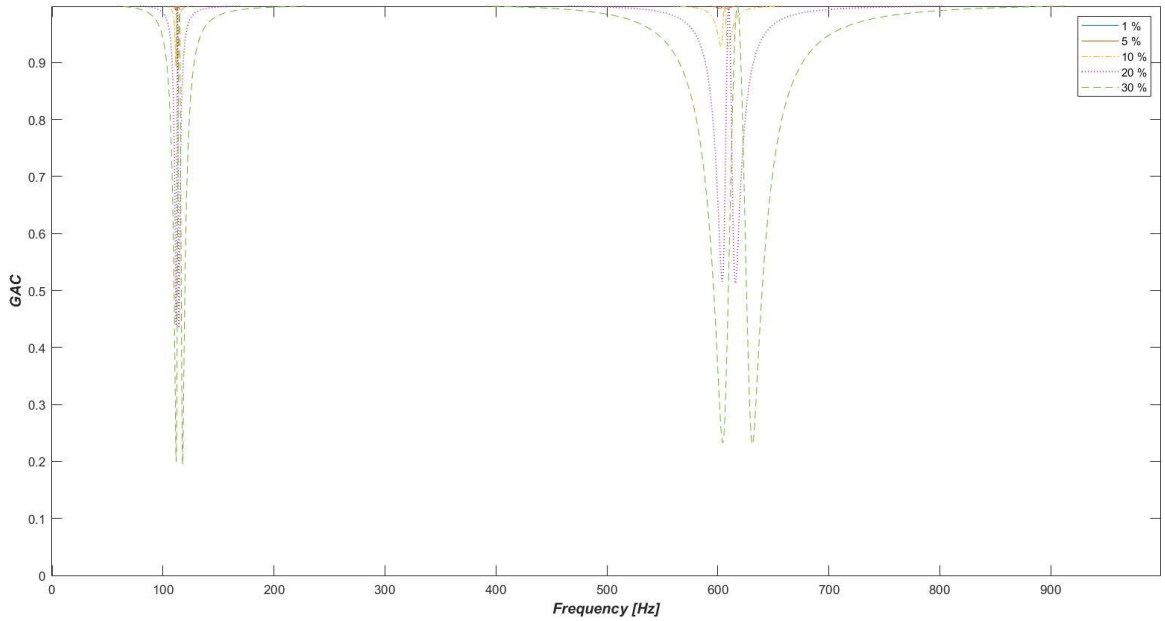

Figure 10: GAC for different crack sizes at node 2.

Figures 8 to 11 show the GSC and GAC indexes for different damage sizes at both nodes. For small damage, around 1% crack size, both GAC and GSC at the two nodes remain at unit value for the frequency band. For more significant damage sizes, values of the two criterions begin decreasing at specific portions of the frequency band. It is possible to see the presence of disturbance between 100 Hz and 200 Hz and between 500 Hz and 700 Hz.

Therefore, it was possible to obtain a global estimation of the beam's structural integrity. For small cracks to the size of 5 %, there was little change, while for cracks greater than 10 %, both worked as good indicators, showing the modes where the damage (crack) exerts greater influence and making way for future analysis of damage detection.

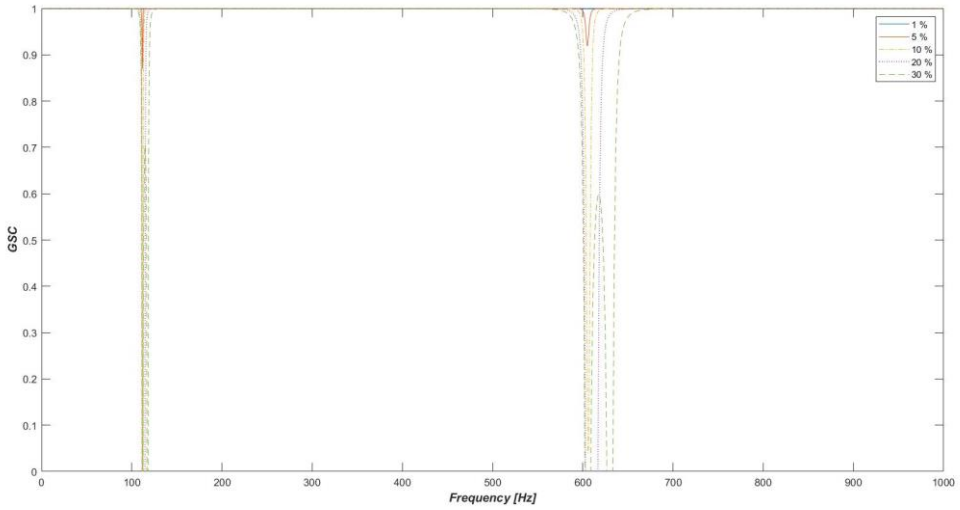

Figure 11: GSC for different crack sizes at node 2

5. CONCLUSION

This paper treats de damage detection regarding the analyzes of the alterations caused in the structural dynamic response due to the damage. The indicators used to compared and monitoring the changes in the response were the called damage indexes. To simulate the dynamic response of a beam, the Spectral element method was used, and six damages index were demonstrated and tested. All indicators showed a sensitive correlated with the crack size. However, the FRAC and FAAC proved to be more sensitive to the crack growing.

6. REFERENCES

Banerjee, S., Ricci, F., Monaco, E., Mal, A., 2009. "A wave propagation and vibration-based approach for damage identification in structural components". *Journal of Sound and Vibration*, Vol. 322, pp. 167-183.

Doebling, S. W., Farrar, C. R., and Prime, M.B., 1998. *A review of vibration-based damage identification methods*. Technical Report, Engineering Analysis Group, Los Alamos National Laboratory, Los Alamos, NM.

Doyle, J. F., 1997. *Wave Propagation in Structures - Spectral Analysis Using Fast Discrete Fourier Transforms*. Mechanical Engineering Series, Springer, New York, 2nd edition.

Krawczuk, M., 2002. "Application of spectral beam finite element with a crack and iterative search technique for damage detection". *Finite Elements in Analysis and Design*, Vol. 38, Issue 6, pp. 537–548.

Monnier, T., 2006. "Lamb Waves-based Impact Damage Monitoring of a Stiffened Aircraft Panel using Piezoelectric Transducers". *Journal of Intelligent Material Systems Structures*, Vol. 17, pp 411-421.

Morassi, A. e Vestroni, F., 2008. "*Dynamic methods for damage detection in structures*". CISM Courses and Lectures, vol. 499. Springer, New York.

Sinou, J., 2009. "A Review of Damage Detection and Health Monitoring of Mechanical Systems from Changes in the Measurement of Linear and Non-linear Vibrations". In *Mechanical Vibrations: Measurement, Effects and Control*, pp. 643–702. Nova Science Publishers.

Su, Z. e Ye, L., 2009. "Identification of Damage Using Lamb Waves". *Lecture Notes in Applied and Computational Mechanics*, Vol. 48. Springer.

Tada, H., Paris, P. and Irwin, G.R., 1973. *The Stress Analysis of Cracks Handbook*. 3rd edition, Del Research Corporation.

Zang, C., Friswell, M.I., Imregun, M., 2003. "Structural Health Monitoring and Damage Assessment Using Measured FRFs from Multiple Sensors, Part I: The Indicator of Correlation Criteria". *Key Engineering Materials Vols*. 245-246, pp. 131-140. Trans Tech Publications, Switzerland.

Zang, C., Grafe, H., & Imregun, M., 2001. Frequency-domain criteria for correlating and updating dynamic finite element models. *Mechanical Systems and Signal Processing*. Vol. 15(1), pp.139–155. https://doi.org/10.1006/mssp.2000.1357.

7. RESPONSIBILITY NOTICE

The authors are the only responsible for the printed material included in this paper.